sustainability

MDPI

Article

Effective Trapping of Pollutants in Fluvisols of the Inter-Embankment Zone of the Odra River Valley (SW Poland)

Dorota Kawałko [1], Joanna Beata Kowalska [1,*], Jarosław Kaszubkiewicz [1], Paweł Jezierski [1], Daria Szuk [1], Mirosław Kobierski [2] and Joanna Gmitrowicz-Iwan [3]

[1] Institute of Soil Science, Plant Nutrition and Environmental Protection, Wroclaw University of Environmental and Life Science, Grunwaldzka 53, 50-357 Wroclaw, Poland; dorota.kawalko@upwr.edu.pl (D.K.); pawel.jezierski@upwr.edu.pl (P.J.); 121288@student.upwr.edu.pl (D.S.)

[2] Department of Biogeochemistry, Soil Science, Irrigation and Drainage, University of Science and Technology, Kaliskiego 7, 85-029 Bydgoszcz, Poland; kobierski@pbs.edu.pl

[3] Institute of Soil Science, Environmental Engineering and Management, University of Life Sciences in Lublin, Leszczyńskiego 7, 20-069 Lublin, Poland; joanna.gmitrowicz-iwan@up.edu.pl

* Correspondence: joanna.kowalska@upwr.edu.pl

Abstract

The aim of this study was to critically assess the usefulness of pollution indicators in monitoring riverside soils (fluvisols) for heavy metal content. A novel methodological approach was used, comparing areas located inside and outside flood embankments, which allowed for a precise determination of the impact of fluvial and anthropogenic processes on heavy metal accumulation. The experimental logic validated the usefulness of four indicators: the Individual Pollutant Index (PI), the Background Enrichment Factor (PIN), the Potential Ecological Risk (RI), and the Pollution Load Index (PLI). Comparative analysis revealed that soils within the embankment zone have higher metal concentrations, resulting from the continuous deposition of alluvial material, which often contains industrial and municipal pollutants. The vertical distribution of pollutants in fluvisols was shown to be closely related to sediment dynamics and soil properties (clay fraction, organic matter, redox conditions). Validation of the indicators revealed their varying sensitivity. The study revealed the limitations of the PLI, which, due to its summary nature, did not account for significant variability in contamination within the soil profile. Consequently, the PI, PIN, and RI indices were shown to be the most effective tools in assessing the actual degree of soil contamination by fluvisols in the middle Oder Valley. The study results emphasise the need for the selective selection of indicators in environmental monitoring. This comparative approach provides a reliable method for assessing the effectiveness of floodplain management strategies under exposure to chemical pressure.

Keywords: industrial pollution; pollution assessment; heavy metal content; gradual sedimentation; stratified soil; fluvisols; sustainable development

Check for updates

Academic Editors: Bo Zhang and Giuseppe Barbaro

Received: 2 March 2026
Revised: 19 May 2026
Accepted: 3 June 2026
Published: 11 June 2026

1. Introduction

For centuries, river valley soils have attracted human interest due to their exceptional utility value and high potential productivity. Alluvial soils also have a special role in the functioning of specific protected natural and semi-natural habitats [1,2]. Stratified alluvial soils, often containing buried topsoil horizons in their profiles, are also important for reconstructing changes including climatic and hydrological changes as well as human impact on the environment [3]. The potential of these soils arises from the dynamic process of alluvial sedimentation, which enriches the profile with organic matter and minerals [4–6]. The deposited sediments exhibit distinct vertical and spatial variation, determined by factors such as the original morphology of the floodplain terrace surface, the source of floodwaters, the time of sedimentation, and land use [7–9]. Furthermore, the number of layers in soil profiles, their arrangement, and spatial extent continue to undergo minor or major transformations during contemporary floods, which introduce new nanoparticles [5,10].

The extensive regulation of the Oder River valley, initiated by straightening the riverbed in the 19th century and building flood embankments in the early 20th century, led to significant environmental and economic changes. A key consequence of this was the separation of a substantial portion of the river's riparian forests. This process was further exacerbated by the opening of a hydroelectric power plant in Brzeg Dolny (1958), which resulted in riverbed erosion and, consequently, a lowering of the groundwater table below the weir [11,12]. The reduction in floods and lowering of the water level facilitated deeper penetration of the soil profile by plant roots, fauna and microorganisms, leading to the development of the cambic subsurface diagnostic soil horizon [13] and modification of the stability of organic matter, which is a crucial factor in maintaining high productivity of alluvial soils under changing environmental conditions [9,14]. The analysis of these transformations aligns with the concept of sustainable development, emphasizing an understanding of the long-term consequences of human activities in river valleys. Knowledge of how soil properties change under the influence of river regulation allows for better forecasting of their resilience to droughts and carbon sequestration processes in the environment. Proper management of these resources is essential to reconcile economic goals with biodiversity conservation and the adaptive capacity of river valleys to global climate change.

Rivers and floodplains are interconnected, enabling the exchange of water, sediments, biota, and nutrients in a shared natural ecosystem. They cover 7% of Europe's total area and perform numerous ecosystem functions, including pollution regulation and acting as sinks for contaminants. Various studies worldwide focus on contaminated floodplains [15–18]. The considerable variability in contaminants, soil properties, and other natural and land-use conditions in floodplains complicates efforts to fully assess soil pollution and related filtration ecosystem services [19]. Soils in river valleys, especially fluvisols, function as strategic biogeochemical sinks. This mechanism is based on the physical sedimentation of polluted suspensions and the chemical sorption of metal ions by active soil components. The unique, distinctive texture of alluvial soils, characterised by the interbedding of silt and clay fractions, creates a multi-level filter that effectively limits the migration of pollutants into the profile and groundwater. The effectiveness of this process is closely linked to the large specific surface area of fine mineral particles, which act as natural sorbents for heavy metals [20]. Thus, the composition of floodplain sediments reflects diverse transport and sedimentation mechanisms, including material transfer directly from the riverbed [21]. These soils often have higher contents of potentially toxic elements. Key sources of contamination include discharges of insufficiently treated sewage, leachates from poorly secured wastewater dumps and historical landfills, and diffuse inflow from catchments [19,22]. Although metals can be transported over considerable distances in dissolved or suspended form, they tend to rapidly precipitate and enrich bottom sediments near the emission source. Such enriched sediments then become a secondary source of pollution [23]. During floods, this material is deposited on floodplains, leading to the accumulation of metals primarily in superficial alluvial soils [20,24]. However, under long-term reducing conditions, deposited pollutants can undergo further remobilization processes [25]. Understanding these processes is crucial for sustainable development,

https://doi.org/10.3390/su18125996

which aims to protect natural resources for future generations by minimizing human impact. Effective management of river valley ecosystems as natural filters helps maintain groundwater purity and food security in agricultural areas.

The issues analysed are directly relevant to the Oder Valley—the second largest river in Poland (Figure 1). In its upper course, the Oder drains the Upper Silesia region, which has been subject to the intensive, centuries-old exploitation of hard coal deposits and zinc and lead (Zn-Pb) ores, as well as a highly developed heavy industry [26–28]. A high degree of anthropopressure also affects the tributaries of the upper Oder, which remain heavily polluted [29,30]. The peak of discharges of saline mine waters and industrial wastewater into the Oder river system occurred in the second half of the 20th century [31]. Numerous studies confirm significant enrichment of sediments in the upper reaches of the river (above Wrocław) with heavy metals. Extensive research on pollutant redistribution has been conducted in this part of the valley, with particular emphasis on geomorphological processes induced by river regulation. It has been demonstrated that highly contaminated sediments, initially deposited in groyne fields, were displaced by modifications to the shoreline and levees, leading to their secondary deposition on floodplains [28,32]. Also, in the lower reaches of the Oder, below Głogów, high accumulation of heavy metals, particularly copper (Cu) and lead (Pb), has been recorded [33–36]. This phenomenon is directly linked to the anthropogenic inflow of pollutants from the Legnica–Głogów Copper District—the largest centre of copper ore mining and processing in Europe [37]. The middle reaches of the Oder are subject to less pressure from pollutants transported from the Upper Silesian Industrial District, although point emission sources may still play a significant role [38,39]. The most important of these sources include municipal and industrial wastewater discharges from the Wrocław metropolitan area as well as the operations of the PCC Rokita chemical plant in Brzeg Dolny, which is classified as a high-risk industrial accident facility.

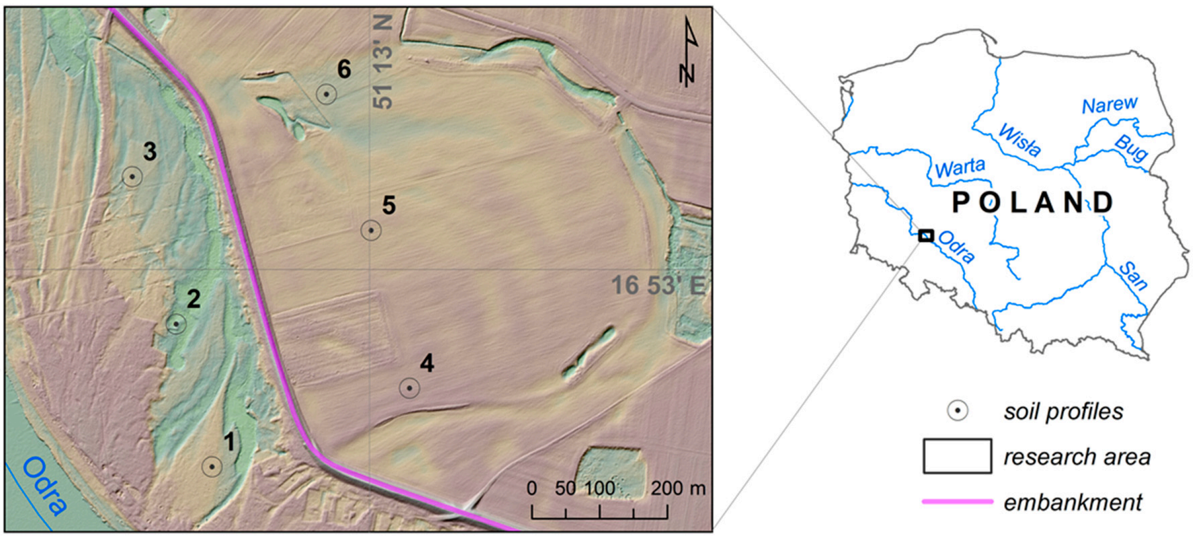

Figure 1. Study area and situation of soil profiles (1, 2, 3. . .6).

Over the past few decades, quantitative geochemical indicators have become a key tool for the objective assessment of anthropogenic environmental pollution by heavy metals [40–42]. Their use enables the distinction between the natural geochemical background from enrichment resulting from human activities, which is essential in monitoring various ecosystems [41]. These indicators have been used to assess the levels of contamination in urban soils [43,44], floodplains [38,45], organic areas [46], polar regions [47] and legally protected territories [48].

The main objective of this study was to assess the accumulation potential of Fluvisols with respect to heavy metals and to verify the hypothesis that they act as a natural geochemical barrier, effectively retaining pollutants transported by the river. A novel methodological approach was used, comparing areas located inside and outside flood embankments, which allowed for a precise determination of the impact of fluvial and anthropogenic processes on heavy metal accumulation. The study tested the hypothesis that periodic flooding of the inter-embankment zone leads to a permanent increase in metal concentrations in topsoil, while the embankment structure shows features of mechanical and sorption barriers that limit their vertical migration. A hypothesis was also formulated that the textural diversity of the sediments and the organic matter content are key factors controlling the spatial distribution of contaminants in the profile. To this aim, metal concentrations and TOC content were compared across different soil profiles, as well as their total reserves in soil layers of a particular depth, taken from two selected areas—the inter-embankment zone and on the embankment. A crucial element of this research is the selection of pollution indicators that will allow for the objective quantification of anthropogenic impacts in the dynamic valley environment. Due to the high sedimentary variability of floodplain sediments, particular attention was paid to determining a representative geochemical background. The research results will serve as a foundation for responsible spatial planning, reconciling economic needs with the requirement to maintain the sustainability and resilience of the natural environment.

2. Materials and Methods

2.1. Study Area and Location of Soil Profiles

The research was carried out in the period from June to September 2022 in the Odra River Valley, in the middle course of the river, downstream from Wrocław (Figure 1). The Pleistocene terraces, shaped by fluvioglacial water from Weichselian glaciation, are mainly composed of sands and gravels, while the Holocene terraces contain fine-textured interbeddings. The top surface layers of floodplains are typically built of loams or silts [49,50]. River channellization and the construction of the embankments in the early 20th century effectively protected the area outside the embankments from flooding and additionally led to the lowering of the groundwater table [12,32]. These changes created favourable conditions for the agricultural use of soils, resulting in the replacement of riparian forests by farmlands, and pastures with ploughed fields. The inter-embankment areas are also used for agricultural purposes, mostly as semi-natural meadows or pastures.

Six soil profiles were selected for this study. The division into the embankment zone and the out-embankment zone is based on the existence of an anthropogenic hydrological barrier, which for decades has radically differentiated these two areas in terms of flooding frequency, fresh sediment deposition and redox conditions. The soil profiles were divided into two groups (for further data interpretation of pollution indices) based on their location in relation to the Odra River, grain size distribution and land use. The first group (Group 1) consisted of profiles P1, P2 and P3, located within the inter-embankment meadow zone and characterised by silt loam and loam textures. The second group (Group 2) included profiles P4, P5 and P6, located outside the embankment in arable fields and characterised by a sandy texture with a loamy in topsoil. All soil profiles were classified and described according to the World Reference Base for soil resources [51].

2.2. Soil Sampling, Analysis and Data Analysis

Research and exploratory drilling were performed in the analysed area. Given the specific nature of the sites (flood embankments), an approach based on representative soil profiles was adopted, foregoing multiple sampling within a single level in favor of thorough homogenization of the material prior to analysis. Based on these drillings, soil excavation sites were then selected to best reflect the spatial variability of the soil cover in the inter-embankment zone and on the embankment. Soil pits were dug to a depth of at least 1.5 m or to the groundwater table. Samples were collected from all morphologically distinguishable horizons and layers. The basic soil properties were determined in representative aliquots of the collected samples. The soil texture was determined using a combined sieve and hydrometer method [52]. Chemical analyses were carried out using standard methods commonly applied in soil science [53] after grinding the soil samples to a fine powder. The soil pH was measured potentiometrically in a suspension in 1 M KCl (soil-to-solution 1:2.5; w/v). A dry combustion method (VarioMacroCube, Elementar, Langenselbold, Germany) was used to determine organic carbon (TOC). The total concentrations of Cd, Cu, Zn and Pb were determined, after soil digestion with aqua regia (concentrated HCl and HNO_3, 3:1 v/v) in a microwave system, according to ISO 11466 [54]. The concentrations of elements in the digests were measured by ICP-AES (iCAP 7400, Thermo Fisher Scientific, Bremen, Germany). The accuracy of the results was verified using two reference materials: CNS 392 and CRM 027, supplied by Sigma-Aldrich, St. Louis, MO, USA), certified for aqua-regia extracted elements. The recovery of elements in CRMs ranged from 82 to 124% for Cd, and from 94 to 109% for the remaining elements, which were considered satisfactory.

As part of the statistical analysis, after checking the normality of logarithmized distributions with the Shapiro–Wilk test ($p < 0.05$), the concentration of metals and TOC at analogous depths was compared using the paired one-sided Student's t-test. The Pearson correlation coefficient between selected variables was analysed. Comparisons of stocks were made for non-logarithmized values using the one-sided unpaired Student's t-test. Statistical analyses were performed using Statistica 13.0 software (StatSoft, Tulsa, OK, USA).

2.3. Pollution Indices

Pollution indices are among the most widely used methods in soil science for assessing potential heavy metal contamination [41,46,48,55–59]. Pollution indices are used to determine whether heavy metal concentrations are sufficiently elevated to indicate potential contamination. In addition to identifying contamination, they enable the assessment of contamination levels, the identification of pollution sources (natural vs. anthropogenic), the evaluation of soil quality and the estimation of potential pollution risks. Moreover, pollution indices are relevant for soil monitoring and supporting long-term soil sustainability [41]. In this study, four pollution indices were applied: the Single Pollution Index (PI) [60], Background Enrichment Factor (PIN) [61], Potential Ecological Risk (RI) [62] and Pollution Load Index (PLI) [41,63]. These indices were chosen because they provide complementary information on contamination levels: the PI and PIN allow the evaluation of individual element enrichment, whereas the PLI and RI provide an integrated assessment of overall site contamination and potential ecological risk. This approach aligns with previous studies highlighting the usefulness of these indices for comprehensive contamination assessment [41].

Detailed descriptions of the indices, including their formulae and classification criteria, are provided in Table A1 (Appendix A). The key elements in the pollution index calculations are (1) the content of heavy metals in soil samples (in individual soil horizons) and (2) the geochemical background [64]. Here, we decided to use the local geochemical background (LGB).

2.4. Geochemical Background

In this study, the so-called LGB was used, which refers to the heavy metal content of a specific site area. The LGB is important for assessing environmental pollution, identifying geochemical anomalies within the soil profile, and understanding regional differences in heavy metal composition [41,65]. Research on the LGB also helps to elucidate the natural processes occurring in a studied region.

The LGB was defined as the average concentration of each heavy metal determined from the deepest soil horizon in which it was detected, with extreme values excluded. This horizon was selected because it is considered the least affected by anthropogenic accumulation and therefore best represents natural conditions. These values were used as the baseline for calculating pollution indices. By reflecting site-specific geological variability, this approach provides a more appropriate reference than generalised background levels, allowing for a clearer distinction between natural and anthropogenic contributions and reducing the risk of misclassifying naturally elevated concentrations as contamination. Pollution indices were calculated for each soil horizon. This allowed us to obtain comprehensive data regarding the pollution of the soil, as well as to assess whether the increase in the level of potential pollution had occurred gradually or was sudden and intense.

In accordance with the divisions adopted in the methodology (based on the grain size distribution, land use and location), the results were also described to enable comparative analysis of the indicator values.

3. Results

3.1. Basic Soil Properties

All soils showed stratification typical of alluvial soils [3,66–68]. The studied soils differed in the morphological features of individual genetic horizons, the depth of the groundwater table, the extent and intensity of redoximorphic features, and the depth and stratification of the alluvial parent material (Figure 2). Based on the WRB Classification [51], soils located in the inter-embankment area (Group 1) were classified as Eutric Gleyic Fluvic Cambisol (Ochric) and Eutric Fluvic Stagnic Cambisol (Ochric) (Figure 3, Tables 1 and 2).

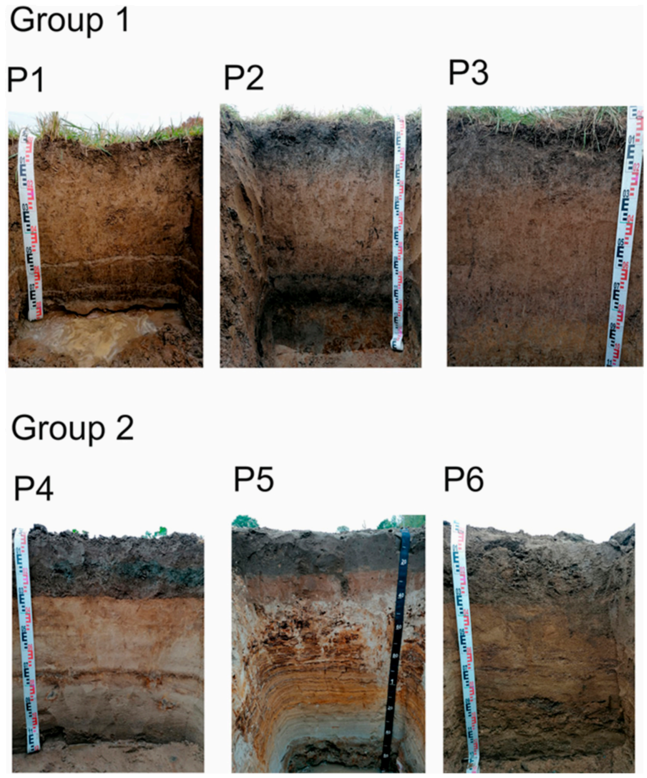

Figure 2. Photographs of the studied soil profiles: P1, P2, P3—located within the inter-embankment zone, P4, P5, P6—located outside the embankment.

Table 1. Soil classification and selected soil properties of the soil from inter-embankment (P1, P2, P3).

Profile Number	Soil Classification [51]	Horizon	Depth (cm)	Munsell Colour Charts	Structure	pH		TOC	N_{tot}	C/N	Sand (2.0–0.05 mm)	Silt (0.05–0.002 mm)	Clay (<0.002 mm)	Textural Classes * [51]
						H_2O	KCl	$g \cdot kg^{-1}$						
P1 In-E	Eutric Gleyic Fluvic Cambisol (Ochric)	Ad	0–10	10YR 3/3	gr	5.0	3.8	28.75	1.85	16	17	59	24	SiL
		ABwg	10–20	7.5YR 4/3	sb	5.3	3.7	15.31	1.02	15	16	62	22	SiL
		Bwg	20–45	10YR 4/3	sb	5.4	3.7	9.18	0.47	20	13	57	30	SiCL
		BCg	45–55	10YR 6/2	sb	5.6	3.8	6.95	0.34	20	12	66	22	SiL
		IIG	55–58	10YR 5/2	ab	5.3	4.1	2.34	n.d.	n.d.	81	13	6	LS
		IIIG1	58–75	2.5Y 5/2	ab	5.2	4.0	6.11	0.35	17	16	63	21	SiL
		IIIG2	75–85	2.5Y 5/2	ab	5.3	4.1	5.80	0.28	21	24	53	23	SiL
		IVG1	85–100	10YR 6/3	sg	5.5	4.7	1.07	n.d.	n.d.	98	1	1	S
		IVG2	100–130	water	sg	5.5	4.5	0.93	n.d.	n.d.	98	1	1	S
P2 In-E	Eutric Fluvic Stagnic Cambisol (Ochric)	Ad	0–18	7.5YR 3/1	gr	5.5	4.8	56.89	2.83	20	24	62	14	SiL
		ABw	18–30	10YR 3/1	sb	5.3	4.5	29.93	2.14	14	27	61	12	SiL
		Bwg1	30–52	10YR 4/3	sb	6.0	4.9	9.44	0.81	12	19	58	23	SiL
		Bwg2	52–80	7.5YR 3/4	sb	5.8	4.8	8.11	0.68	12	32	52	16	SiL
		BCg	80–100	10YR 4/4	sb	6.0	5.0	7.54	0.56	13	36	45	19	SiL
		IICg1	100–113	10YR 4/1	ab	6.1	4.9	7.56	0.48	16	46	29	25	L
		IICg2	113–122	7.5YR 5/8	ab	5.9	4.8	11.51	0.84	14	21	39	40	CL
		IICgg	122–135	10YR 5/1	sb	6.0	4.8	3.49	0.18	19	60	24	16	SL
		IIICgg	135–150	10YR 5/2	sb	6.2	5.1	1.88	n.d.	n.d.	86	6	8	LS
P3 In-E	Eutric Fluvic Stagnic Cambisol (Ochric)	Ad	0–18	10YR 3/1	gr	5.3	4.6	54.16	2.78	19	24	60	16	SiL
		ABw	18–28	10YR 3/3	gr	5.4	4.6	27.52	1.70	16	24	54	22	SiL
		Bwg1	28–40	10YR 4/4	sb	5.8	4.8	9.45	0.72	13	34	47	19	L
		Bwg2	40–70	10YR 4/3	sb	6.0	4.9	7.67	0.65	12	22	58	20	SiL
		Bwg3	70–86	10YR 4/1	sb	6.1	4.7	8.14	0.71	11	27	48	25	SiL
		Cg	86–103	10YR 5/1	sb	5.9	4.4	3.75	0.27	14	34	44	22	L
		IICg	103–150	7.5YR 5/6	sb	5.9	4.6	1.73	0.09	19	74	16	10	SL
		IIIG	150–175	7.5YR 3/4	sg	6.0	4.8	1.65	0.05	33	84	5	11	LS
		IVCgg	175–190	7.5YR 4/6	sg	6.3	5.3	0.66	n.d.	n.d.	98	1	1	S

Explanation: gr—granular; sb—subangular blocky; ab—angular blocky; sg—single grain; LS—loamy sand; S—sand; L—loam; CL—clay loam; SL—sandy loam; SiL—silt loam; SiCL—silty clay loam; In-E—inter-embankment; Out E—out of embankment; * according to the WRB classification; n.d.—not detected.

Table 2. Soil classification and selected soil properties out of the embankment (P4, P5, P6).

Profile Number	Soil Classification [51]	Horizon	Depth (cm)	Munsell Colour Charts	Struktura	pH		TOC	N_{tot}	C/N	Sand (2.0–0.05 mm)	Silt (0.05–0.002 mm)	Clay (<0.002 mm)	Textural Classes * [51]
						H_2O	KCl	$g \cdot kg^{-1}$						
P4 Out E	Eutric Stagnic Fluvisol (Katoarenic, Ochric, Brunic)	Ap	0–30	10YR 4/2	gr	6.4	5.4	11.50	0.98	12	57	25	18	SL
		IIBvg	30–45	10YR 4/4	sb	6.1	5.1	2.45	0.09	27	94	2	4	S
		IIBvCg	45–60	10YR 5/4	sg	6.3	5.2	2.33	0.03	78	95	2	3	S
		IICg1	60–72	10YR 5/3	sg	6.3	5.2	0.64	0.01	64	98	0	2	S
		IICg2	72–78	10YR 4/3	sb	6.2	4.9	1.99	0.05	40	81	13	6	LS
		IICg3	78–110	10YR 6/3	sg	6.4	5.3	0.55	n.d.	n.d.	99	0	1	S
		IICgg	110–150	10YR 5/2	sg	6.4	5.5	0.72	n.d.	n.d.	98	0	2	S
P5 Out E	Eutric Stagnic Fluvisol (Katoarenic, Ochric, Brunic)	Ap	0–24	10YR 3/2	gr	6.6	5.5	8.82	0.31	28	73	22	5	SL
		ABv	24–40	10YR 4/3	sg	4.7	3.8	3.32	0.09	37	75	21	4	LS
		IICrg1	40–60	10YR 6/2	sg	5.5	4.6	1.33	n.d.	n.d.	93	5	2	S
		IICrg2	60–90	5YR 4/6	sg	6.5	5.3	1.21	n.d.	n.d.	93	3	4	S
		IICrg3	90–115	10YR 6/6	sg	6.5	5.1	0.48	n.d.	n.d.	93	3	4	S
		IIG	115–150	5Y 7/2	sg	6.3	5.3	0.47	n.d.	n.d.	92	4	4	S
		IIIG	150–180	5Y 6/2	m	6.5	5.0	1.31	n.d.	n.d.	72	15	13	SL
P6 Out E	Eutric Stagnic Fluvisol (Katoarenic, Ochric, Brunic)	Ap	0–33	10YR 4/3	gr	5.8	4.8	11.47	0.97	12	52	31	17	SL
		IIBv	33–55	10YR 3/4	sb	6.7	5.6	3.39	0.21	16	82	11	7	LS
		IICg1	55–70	10YR 4/4	sg	6.7	5.5	0.88	n.d.	n.d.	99	0	1	S
		IIC2	70–90	7.5YR 4/4	sg	7.0	5.8	0.81	n.d.	n.d.	99	0	1	S
		IIC3	90–110	7.5YR 4/6	sg	6.8	5.7	0.78	n.d.	n.d.	98	0	2	S
		IIC4	110–150	7.5YR 4/4	sg	7.0	5.8	0.61	n.d.	n.d.	98	0	2	S

Explanation: gr—granular; sb—subangular blocky; m—massive; sg—single grain; LS—loamy sand; S—sand; SL—sandy loam; In-E—inter-embankment; Out E—out of embankment; * according to the WRB classification; n.d.—not detected.

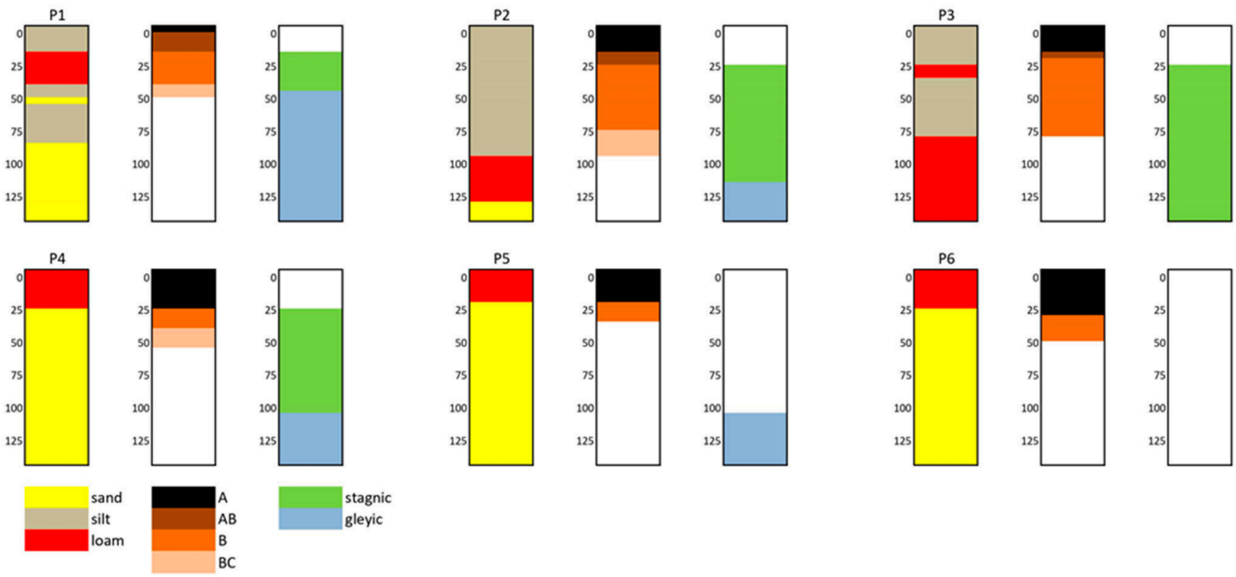

Figure 3. Selected morphological features of the studied soils: texture layering in the soil profiles; thickness of A, AB, B and BC horizons (in centimetres); the presence and depth of stagnic and gleyic properties (in centimetres); P1, P2, P3—profiles located within the inter-embankment zone, P4, P5, P6—profiles located outside the embankment.

The soils were characterised by a fine silty-loam texture. A sandy substrate was detected below the depth of 85 cm. The humus horizon, dark in colour and exhibiting a granular structure, was 10–18 cm thick. The content of total organic carbon (TOC) in these layers ranged from 28.75 to 56.89 $g \cdot kg^{-1}$. Furthermore, there was a well-developed Bwg horizon with a subangular blocky structure and transitional ABwg and BCg horizons in these soils, indicating the intensive development of the cambic horizon. In all soils located in the inter-embankment zone, from a depth of about 28 cm, stagnic features were observed. In most profiles, gleyic features were also visible at greater depths due to the influence of groundwater. The soil pH values measured in suspension in H_2O ranged from 5.0 to 6.3. These soils were characterised by a much higher TOC content and slightly lower pH values compared to the soils outside the embankment area, which may be related to their use as meadows.

Soils located outside the flood embankments (Group 2) were classified as Eutric Stagnic Fluvisol (Katoarenic, Ochric, Brunic). These were soils with a sand texture and a loamy topsoil. The humus horizon, dark in colour and granular in structure, was 24–33 cm thick, and the TOC content ranged from 8.82 to 11.50 $g \cdot kg^{-1}$. In the soil profile of these soils, a diagnostic horizon Bv with a subangular blocky structure or the transitional horizons ABv and BvC with a single grain structure were identified. In some soil profiles, stagnic features were visible in the middle part of the profile, or gleyic features were observed at a depth of more than 100 cm (Figure 3). No reductomorphic features were found in one profile (P6). The pH values of these soils measured in suspended H_2O ranged from 4.7 to 7.0 (Tables 1 and 2).

3.2. Metals in Soil Profiles

The risk associated with soil contamination was assessed according to Polish legal regulations [69,70], which differentiate permissible concentrations of contaminants according to the categories of soil usage and land use. In the case of farmland topsoils (0–25 cm), the permissible concentrations of metal(loid)s depend on soil texture and pH. In deeper layers (>25 cm), they are only related to soil water permeability. The metal concentrations in the analysed soil samples differed significantly between both soil groups (Table A2, Appendix B). In the soils within the embanked area (group 1), the concentrations ranged from

0.4 to 2.36 mg·kg^{-1} for Cd (the permissible value is 3 mg·kg^{-1}), from 1.35 to 41.1 mg·kg^{-1} for Cu (the permissible value is 150 mg·kg^{-1}), from 3.35 to 263 mg·kg^{-1} for Zn (the permissible value is 500 mg·kg^{-1}), and from 1.41 to 51.02 mg·kg^{-1} for Pb (the permissible value is 250 mg·kg^{-1}) [69]. The topsoil in Ad contained higher concentrations of metals. This group of samples was also the richest in TOC, which was likely primarily driven by their use as a meadow (Tables 1 and 2).

Soils located outside the embankment (Group 2) were characterised by significantly lower enrichment in metals both at the surface and in deeper layers (Table S2, Supplementary Material). The concentrations of the analysed elements ranged from 0.40 to 0.95 mg·kg^{-1} for Cd (the permissible value is 2 mg·kg^{-1}), from 0.38 to 9.38 mg·kg^{-1} for Cu (the permissible value is 100 mg·kg^{-1}), from 2.35 to 39.9 mg·kg^{-1} for Zn (the permissible value is 300 mg·kg^{-1}), and from 1.21 to 19.57 mg·kg^{-1} for Pb (the permissible value is 100 mg·kg^{-1}) [69]. The highest concentrations were also recorded in topsoils. The permissible concentrations of metals in arable soils were not exceeded in any of the analysed soil profiles. A detailed analysis of the distribution of potentially toxic metals in the soils of the middle Odra floodplain was presented in a previous publication [39].

A comparison of heavy metal contents across the studied sites was difficult due to the high profile variability and associated lack of normality in the distributions of the analysed variables. To overcome these limitations, a two-stage statistical procedure was used. In the first stage, a logarithmic transformation of the data on metal concentrations at individual depths was performed. The normality of the transformed variable distributions was verified using the Shapiro–Wilk test. For the Cu, Pb and Zn concentrations, as well as total organic carbon (TOC), there was no basis on which to reject the null hypothesis of normality.

Therefore, the logarithmized values of the studied parameters were used in the subsequent analysis. Comparisons were made for the mean values calculated for both objects at corresponding depths, treating data from individual profiles as replicates. The significance of differences between objects was assessed using a one-sided Student's t-test for dependent samples. The significance level was $p = 0.05$.

The results of the analyses showed that soils from the inter-embankment zone, in most of the analysed horizons, were characterised by significantly higher concentrations of Cu, Zn and Pb compared to soils from the embankment area. Significant differences for Cu and Zn were noted at 4 of the 6 analysed depths, while for Pb, they were noted at 5 of the 6. A different pattern was observed for Cd, with statistical significance observed only in the shallowest horizons (Tables A3–A6, Appendix C).

A similar trend, as in the case of Cu, Pb and Zn, was observed for TOC content—significantly higher values were recorded at 4 of the 6 depths analysed (Table A3, Appendix C). In none of the analysed cases was the described trend reversed—the average metal concentrations and TOC content were consistently higher in the soils of the inter-embankment zone than in the soils outside of the embankment area.

A strong correlation was observed between TOC content and heavy metal concentrations in the studied soils from both locations. The coefficients of the correlations between selected variables are summarised in Tables A4–A6. Table A4 presents the correlation coefficients for the inter-embankment area, Table A5 for the embankment area, and Table A6 for both areas combined. All correlation coefficients were calculated for logarithmic values.

Statistically significant correlations (at the $p = 0.05$ level) are marked in red. The analysis revealed significant relationships between metal concentrations and TOC content, as well as between individual metals. Significantly lower correlation coefficients (statistically insignificant at the assumed level) were observed only for cadmium in relation to other metals (Cu, Zn, Pb) in the inter-embankment area. Combined with the uniform cadmium concentration throughout the profile, this may indicate its primarily lithogenic origin and weaker affinity for organic matter [71].

An attempt was also made to assess and compare the stocks of the studied heavy metals in both soil groups. For this purpose, the total content of Cd, Cu, Zn, Pb and organic carbon (TOC) was calculated in the 0–50 cm, 50–100 cm and 100–150 cm layers for a unit area of 1 m^2. The calculations assumed a soil bulk density of 1.2 $g \cdot cm^{-3}$ in the accumulation horizons and 1.4 $g \cdot cm^{-3}$ in the remaining horizons. Calculations were performed on raw (non-logarithmic) data to obtain results in absolute units: mg for heavy metals and g (or kg) for TOC (Table A7, Appendix D). To compare the concentrations of individual metals and TOC in soil layers at a specific depth, a paired *t*-test was used for variables without replicates, with a significance level of $p = 0.05$.

Statistically significant differences (at a significance level of $p = 0.05$) are highlighted in red. The analysis showed that, in all the identified layers, the stocks of heavy metals and organic carbon (TOC) are higher in the inter-embankment soils than in the soils outside the embankment. These differences are statistically significant for the 0–50 cm and 50–100 cm layers but are no longer statistically significant in the 100–150 cm layer. The exception is cadmium, for which a significant difference was noted only in the surface layer (0–50 cm).

According to the authors, such a distribution of resources confirms, on the one hand, the affinity of metals to organic matter (OM), and on the other hand, it indicates a more intense accumulation of OM in the inter-embankment area resulting from external supply by deposited alluvial material.

3.3. Pollution Assessment Results

3.3.1. Single Pollution Index (PI)

Group 1 (P1, P2, P3)

The obtained PI values showed generally higher pollution levels in Group 1 than in Group 2. Soil P1 showed very strong Pb pollution at up to a 20 cm depth, which then gradually decreased up to 58 cm, where an absence of Pb pollution was noted. In the case of Zn, a very strong level of pollution prevailed within the first 85 cm. At the depth of 55–85 cm, an abruptly low level of Zn pollution was identified, suggesting the insertion of foreign material. From 85 cm, an absence of Zn pollution was noted. A very similar distribution of pollution was noted for Cu; however, at the depth of 55–85 cm, moderate pollution levels were noted. In the case of Cd, soils to a 100 cm depth showed low PI, below which an absence of Cd pollution was noted (Figure 4).

Soil P2 showed very strong pollution with Pb up to 52 cm and between 113 and 122 cm, and strong pollution up to 113 cm for Pb. Below this depth, moderate and low PI levels were obtained. In analysing the Zn pollution distribution, a very strong PI level was noted up to 122 cm, with a strong and moderate class of pollution found below this depth. The complex distribution of pollution classes was also typical for Cu and Cd, for which very strong levels of pollution were indicated up to 30 cm, as well as between 113 and 122 cm depths. Within soil P2, strong pollution with Cu and Cd was detected between 30 and 113 cm, while only moderate and low levels of pollution were reported below 122 cm (Figure 4).

Soil P3 showed very strong Pb pollution up to 40 cm and strong pollution thenceforth. An insertion of very strongly Pb-polluted soil material was noted at the depth of 70–103 cm, below which low Pb pollution levels and even an absence of Pb pollution with Pb were observed. In the case of Zn, very strong pollution was indicated across almost the whole P3 soil profile (up to 103 cm). In the lowermost horizons, low and absent levels of Zn pollution were identified. Similarly, Cu pollution appeared to decrease with depth, being very strong up to 70 cm and absent at the bottom of the soil profile. However, in the case of Cd, very strong pollution was found only up to 28 cm deep. The majority of soil horizons showed low Cd pollution (28–103 cm) and its absence from 103 to 175+ cm.

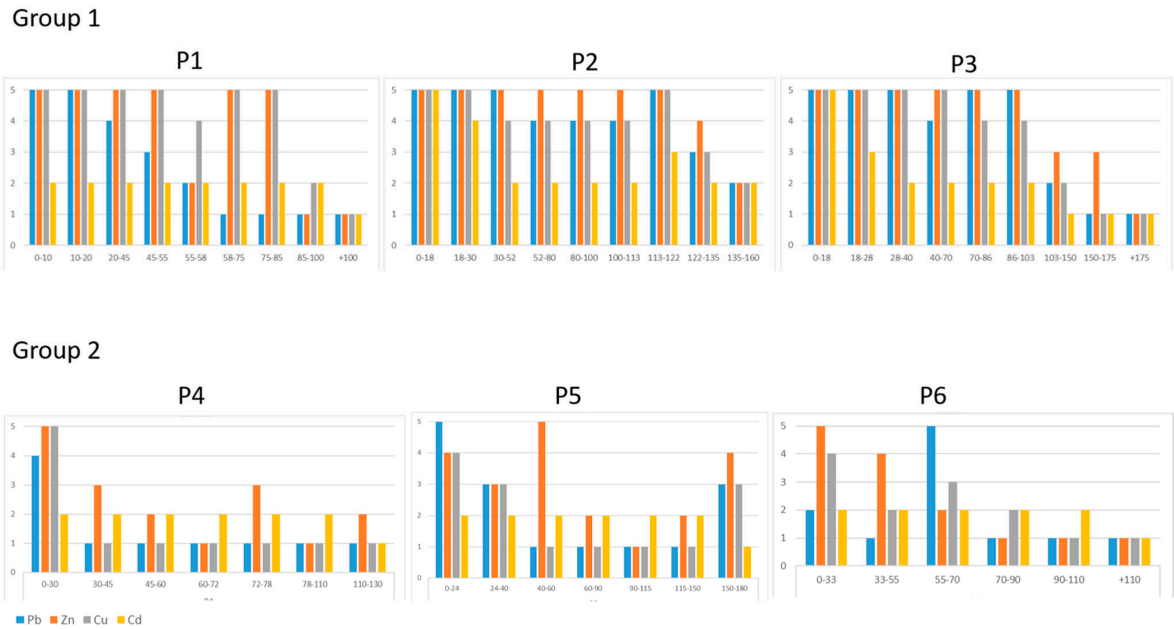

Figure 4. Single Pollution Index (PI) classes according to the different background used. **Explanation: 1 (PI < 1)—absent**; **2 (1 < PI < 2)—low**; **3 (2 < PI < 3)—moderate**; **4 (3 < PI < 5)—strong**; **5 (PI > 5)—very strong**. All PI classes were calculated based on the LGB values. The horizontal axes show the depth of soil horizons within the profile (cm).

Group 2 (P4, P5, P6)

The PI values generally showed a decrease in soil pollution towards the bottom of the soil profile. For soil P4, strong Pb pollution was indicated only in the surface horizon (0–30 cm), below which an absence of pollution was detected (Figure 4). When analysing Zn, very strong pollution was typical for the surface horizon (0–30 cm), whereas alternately moderate–low–absent classes of pollution were found in the lower horizons. The PI calculated for Cu suggested very strong pollution on the surface (0–30 cm) and an absence of pollution in other horizons, while for Cd, low pollution was noted up to 110 cm, below which there was an absence of pollution.

Soil P5 showed a more complex distribution of pollution. The PI calculated for Pb indicated very strong (0–24 cm) and moderate (24–40 cm) levels of pollution, and then low and 'absent' pollution was noted before moderate pollution was detected again at the bottom (150–180 cm). The distribution of Zn pollution was very complex, being strong (0–24 cm), moderate (24–40 cm) and very strong (40–60 cm), followed by low pollution and an absence of pollution until strong pollution was again detected at the bottom of the soil profile (150–180 cm). In the case of Cu, the pollution clearly decreased with depth, from strong pollution on the surface (0–24 cm) to the absence of pollution in the deeper parts of the profile. However, once again, strong pollution was noted in the lowermost horizon (150–180 cm). The PI distributions of Pb, Zn and Cu suggest an allochthonous input at a depth of 150–180 cm, as indicated by unexpectedly high pollution levels. In the case of Cd, low pollution was noted up to 150 cm, below which an absence of pollution was found (Figure 4).

The PI levels calculated for Zn and Cu in P6 showed a decrease in pollution levels with soil depth. In the case of Zn, very strong and strong pollution were indicated at the depth of 0–33 cm, with an eventual absence of pollution at the bottom of the soil profile. Similarly, the classes of PI calculated for Cu showed strong pollution on the surface (0–33 cm), then low and moderate (55–70 cm) pollution, and finally an absence of pollution at the bottom. The distribution of pollution classes for Pb, however, was unexpected: low pollution was noted at a 0–33 cm depth and very strong pollution at a 55–70 cm depth. However, mostly, an absence of pollution was noted below this point. For Cd, low pollution was noted up to 110 cm, below which an absence of pollution was detected (Figure 4).

3.3.2. Background Enrichment Factor (PIN)

Group 1 (P1, P2, P3)

Within soil P1, the 'contaminated' PIN class was indicated between 0 and 45 cm. Most of the horizons, however, were in the 'lightly contaminated' PIN class, although an insert at the depth of 55–58 cm obtained the 'trace contamination' PIN class. The bottom of the soil profile was 'clean'. The PIN values suggested that soil P2 was 'contaminated' at 0–30 cm, 'lightly contaminated' from 30 to 135 cm, and then had only 'trace contamination' thereafter. A very similar pattern of PIN classes was noted in P3: 'contaminated' (0–26 cm), 'lightly contaminated' (26–103 cm) and 'trace contamination' (to the bottom of the soil profile) (Figure 5).

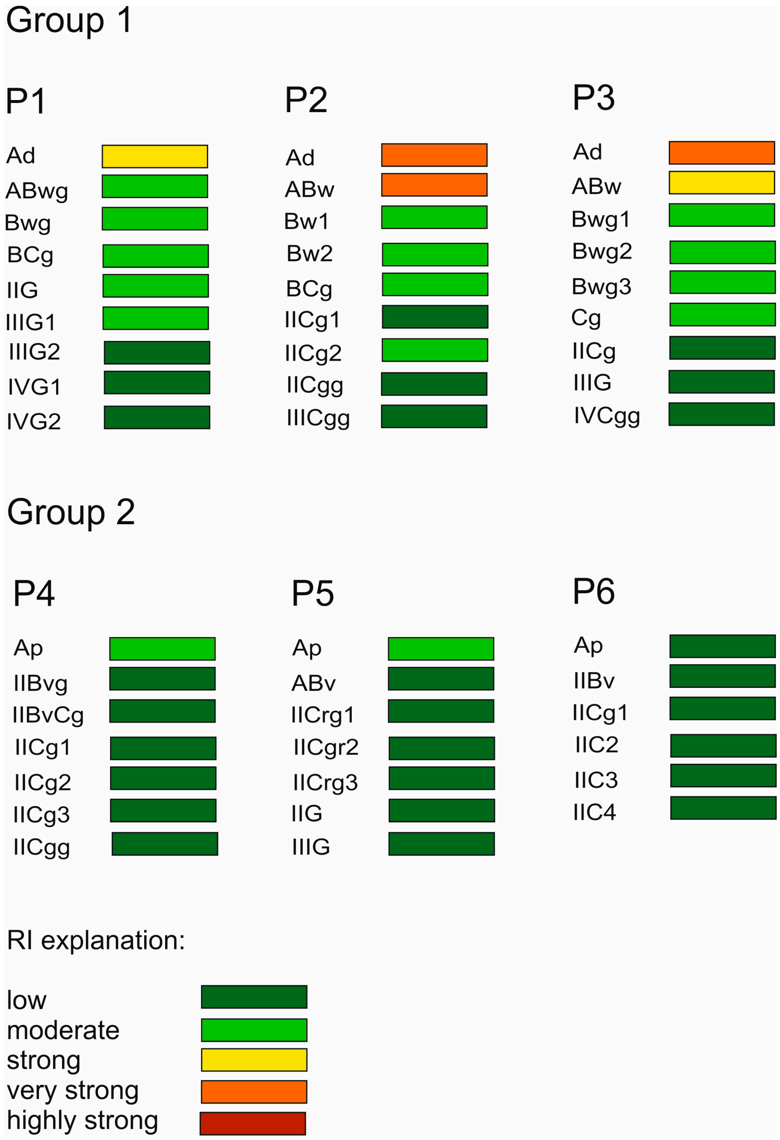

Figure 5. Spatial distribution of Background Enrichment Factor (PIN) classes in the studied soils, illustrating variations in element enrichment across soil horizons. **Explanations: P1, P2, P3—located within the inter-embankment zone, P4, P5, P6—located outside the embankment**.

Group 2 (P4, P5, P6)

The top horizon of P4 (0–30 cm) showed light contamination before decreasing to trace contamination and even 'clean' soil towards the bottom of the profile (Figure 5). In soil P5, the PIN classes were distributed unevenly, with light contamination on the surface (0–24 cm), in the middle (40–60 cm) and also at the bottom (150–180 cm), as well as trace contamination and 'clean' soil being indicated. Similarly, in soil P6, light contamination was identified at the surface (0–33 cm) and in the middle (55–70 cm) part of the solum, besides which trace contamination and 'clean' soil were reported.

3.3.3. Potential Ecological Risk (RI)

Group 1 (P1, P2, P3)

The surface horizon of P1 (0–10 cm) showed strong potential ecological risk. The RI values indicated lower potential ecological risk in the lowermost horizons of P1, with moderate values up to 85 cm and low values towards the bottom of the soil profile. Soil P2 was characterised by very strong potential ecological risk up to 30 cm in depth. Below 30 cm, the RI values indicated moderate and low potential ecological risk. However, the potential ecological risk decreased with the soil depth in profile P3, showing very strong and strong levels at 0–18 cm and 18–28 cm, respectively. For the majority of the horizon of soil P3, moderate potential ecological risk (28–103 cm) was indicated (Figure 6).

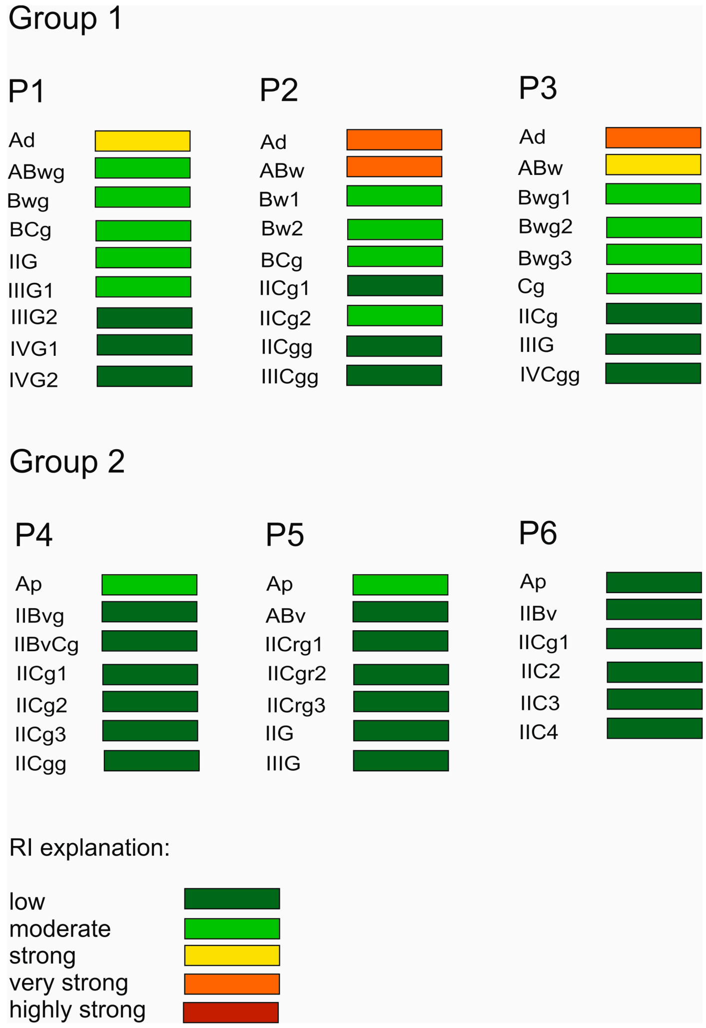

Figure 6. Degree of contamination in the studied soils based on the Potential Ecological Risk (RI), highlighting differences in ecological risk levels across soil horizons. Explanations: P1, P2, P3—located within the inter-embankment zone, P4, P5, P6—located outside the embankment.

Group 2 (P4, P5, P6)

The RI values in the majority of Group 2 samples suggested low potential ecological risk. Only the surface horizon (0–30 cm) of P4 indicated moderate potential ecological risk when using LGB (Figure 6).

3.3.4. Pollution Load Index (PLI)

All the studied soils from both Groups 1 and 2 indicated a deterioration in soil quality according to PLI classes (Figure 7).

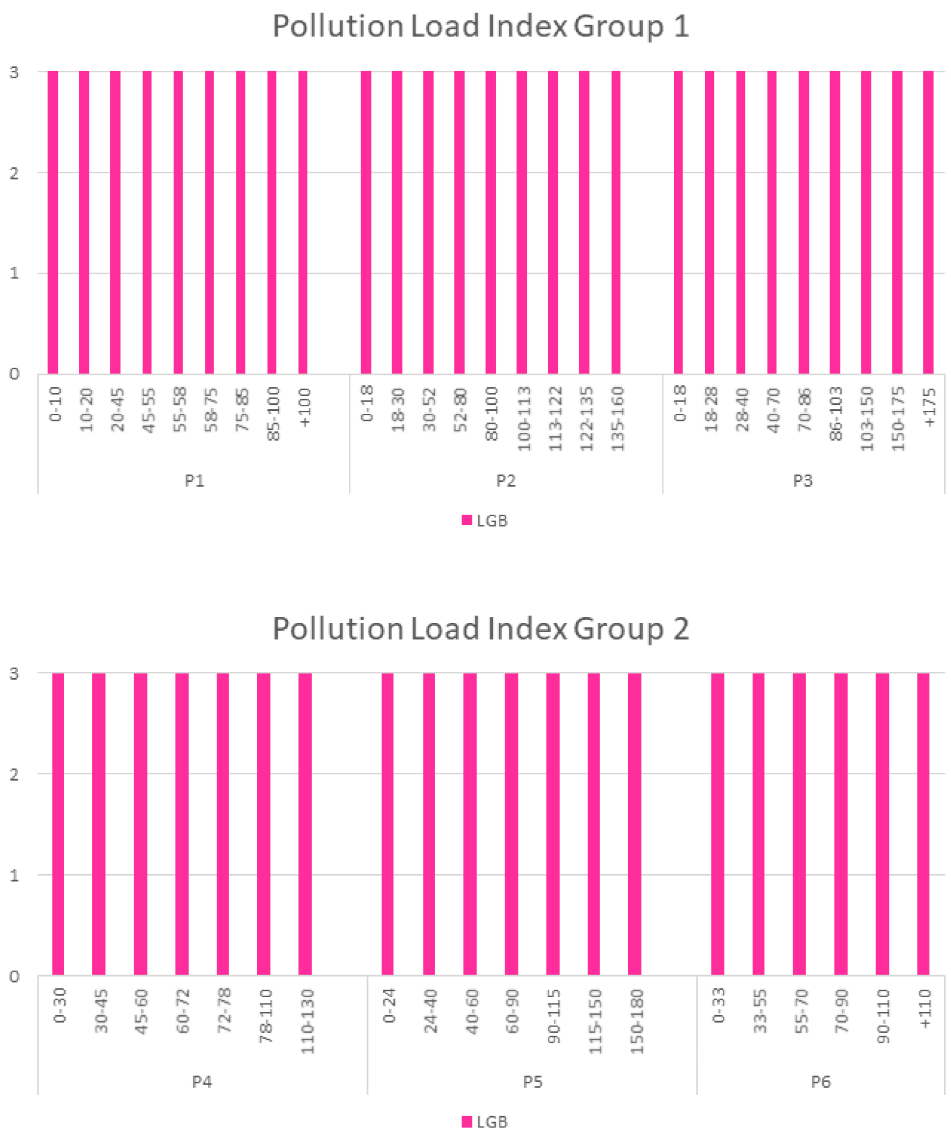

Figure 7. The degree of contamination based on the Pollution Load Index (PLI). Explanation: 1 (<1)—perfection; 2 (=1)—only baseline levels of pollution; 3 (>1)—deterioration in soil quality. The horizontal axes show the depth of the soil horizons within the profile (cm). **Explanations:** P1, P2, P3—located within the inter-embankment zone, P4, P5, P6—located outside the embankment.

4. Discussion

The specificity of fluvisols, whose genesis is inherently related to the gradual deposition of mineral sediments by watercourses such as rivers, is characterised by variability in chemical and physical properties [7–9,72] as well as spatial differentiation of heavy metal content in the soil profile [36,39,73]. This phenomenon has also been confirmed in the present study (Table S2), firstly through a frequent lack of the expected trend in the distribution of heavy metals in the soil profile, where the highest values are recorded in surface horizons—e.g., due to anthropogenic activity—and the content gradually decreases towards the bottom of the soil profile. A similar lack of this trend was also reported in other studies [74–76]. Secondly, the results of this study suggested the possible accumulation of so-called inserts of finer and firmer (e.g., silty-loam or loam-textured) mineral material with a higher content of heavy metals compared to the layers located below and above them. Such inserts were also noted in previous studies [22,77,78]. Furthermore, the deposited sediments in the present study showed clear differentiation in both vertical and spatial arrangements. This is determined by, among other factors, the nature of floodwaters, which carry pollution from anthropogenic sources, such as sewage from mining or industrial areas [28,32].

This study found similar trends in the Odra River Valley, where the content of heavy metals clearly indicated that the level of pollution was higher within the soils of Group 1 samples, which were located in the inter-embankment area (Table S2). The higher heavy metal contamination in soils from the inter-embankment areas was also clearly confirmed by the calculated pollution indices, such as the PI (Figure 4)—particularly in the case of Pb and Cu—as well as complex pollution indices such as the PIN (Figure 5) and RI (Figure 6). The tendency to accumulate pollutants rich in heavy metals in the inter-embankment areas is primarily related to the genesis of fluvisols formed from sediment deposits carried by the Odra River. These fluvisols often exhibit unique characteristics due to their dynamic nature and constant interaction with water bodies, through which they incorporate pollutants [39,73]. As a result, they can act as both sinks and sources of pollutants, depending on various factors such as sediment transport, land use practices and hydrological conditions. Moreover, fluvisols within the inter-embankment area may serve as natural sinks, effectively trapping and immobilising pollutants present in runoff or groundwater before they reach adjacent waterways [79,80]. On the other hand, lower heavy metal contamination may be recorded in the embankment (as noted in soils from Group 2) due to the cutting off of the inflow of pollutants and the lack of mineral sediment deposition by the river as a result of the presence of embankments [78], as reflected in the PI, PIN and RI values (Figures 4–6).

Analysing the PI values (Figure 4), it can be concluded that heavy-metal-rich pollutants had accumulated gradually; this is especially visible in the case of soils from Group 1, where higher PI values for Pb, Zn, Cu and Cd (Figure 4) were often characteristic of surface horizons. This is inherently related to the genesis of fluvisols, that is, the steady accumulation of mineral deposits at different times and of different thicknesses, often rich in anthropogenic pollutants [5,6]. A similar tendency was indicated by the PIN results (Figure 5), in which most of the surface horizon of soils from Group 1 belonged to the 'contaminated' class. Here, the source may be anthropogenic pollutants rich in heavy metals, received by the Odra River. However, Upper Silesia is a region of historical and modern hard coal and Zn-Pb ore mining and heavy industry, which may have led to the tributaries of the upper Odra River becoming heavily polluted with heavy metals [26,27]. Furthermore, the spur fields filled with heavily polluted sediments were cut by new shorelines, and their material was partially forced into the floodplains of the upper Odra River [28,32]. It is worth mentioning that the Odra River is the receiver of local pollution from water discharges from the city of Wrocław and from the PCC Rokita Plant in Brzeg Dolny, recognised as a high-risk chemical plant that may be an additional source of heavy metal in the studied fluvisols [32,38,39]. Furthermore, the sediments forming the surface horizons of soil in this part of the embankment zone were deposited during the last twenty years, probably during hydrotechnical works [20] that could also have created favourable circumstances for enriching the surface layers with pollutants rich in heavy metals. Finally, the construction of the hydroelectric power station in Brzeg Dolny caused a drop in the Odra riverbed level, leading to a reduction in the groundwater table beneath the weir [11,12] as well as the accumulation of pollution [9,14].

Of course, the absorption of pollutants in soils, especially those of such a specific origin as fluvisols, is supported by physical properties. The texture of the deposited material plays a key role in determining its adsorption properties [78,81]. Sediments with coarse grains have a reduced capacity to adsorb contaminants, whereas those with finer grains possess a larger specific surface area and higher ability to adsorb cations, resulting in significantly greater binding of heavy metals [78]. In accordance with the above, the soils of Group 1 (inter-embankment areas) that were characterised by a fine-particle texture (silt loam, loam, Figure 3, Table 1, Table 2) were prone to accumulating more heavy-metal-rich pollutants during mineral sediment accumulation [5,75,82].

As indicated by previous studies [22,45,75,78], the redox potential influences the behaviour of heavy metals in fluvisols and contributes to variations in heavy metal contamination levels, as observed in the inter-embankment zone and out of the embankment areas in the soils under investigation. The occurrence of stagnic/gleyic properties (Table 1, Table 2, Figure 3) in the studied soils within the inter-embankment area indicates that reducing conditions do occur there, and therefore the risk of releasing reducible forms of potentially toxic elements that favour the accumulation of heavy metals in soils is very high [15,72,75,76]. Moreover, the horizons enriched with heavy metals also had a significant content of TOC (reaching up to 56.9 $g \cdot kg^{-1}$ within the soils of the inter-embankment areas). The relation between the TOC and heavy metal accumulation has also been reported by other authors studying fluvisols [45,78] due to the affinity of bioavailable forms of heavy metals for the content of organic matter. Additionally, the slightly lower pH values of soils from the inter-embankment areas compared to those out of the embankment environments may facilitate the dissolution of heavy metals and their transfer into the soil solution, potentially leading to higher pollution levels [75,83].

Moreover, in analysing the PI values, surface soil horizons in soils from the inter-embankment area showed exceptionally high Pb pollution (Figure 4). Although anthropogenic pollution undoubtedly has a direct impact here, it should be emphasised that the Pb profile distribution of elements can be significantly influenced by soil properties and soil processes as mentioned above, as well as by the character of this element [83]. As Pb is considered relatively immobile [84,85], the relationships between the concentrations of various elements of the same origin in soils may differ along the course of the river.

Indeed, chemical and physical properties enable the differentiation between layers of polluted material situated within soil material characterised by comparatively lower levels of contamination. In this study, such layers were identified in soil P1 (horizons IIIG1, IIIG2), P5 (horizon IICrg1) and P6 (horizon IICg1) based on PIN classes (Figure 5). Due to the nature of fluvisols, which are characterised by the gradual deposition of mineral material (sedimentation) with varying properties (e.g., content of TOC, fine-textured grain size distribution) and ages, some of the deposited horizons may exhibit higher pollution levels, as confirmed by PIN. Often, a one-time pollution discharge into water or the periodic intensification of industrial activities can influence the heavy-metal-rich contamination of the given soil layer(s) [74] as the polluted river water easily infiltrates into the gravelly and sandy sediments typical of fluvisols.

Based on the PLI (Figure 7) indices, which focus on comprehensive soil contamination with all studied heavy metals, soils located in both the inter-embankment area and those out of the embankment exhibited a deterioration in soil quality, with quite similar pollution classes in both cases. Although the Pollution Load Index (PLI) indicated a deterioration in soil quality in all the studied soils from both Groups 1 and 2, it did not reflect the variability of contamination observed within soil profiles (Table S2). This limitation is related to the mathematical structure of the index. The PLI is calculated as the geometric mean of individual pollution indices, which inherently reduces the influence of extreme values. As a consequence, high or low values of particular elements are moderated, leading to a smoothing effect. While this property makes the PLI useful for providing an overall assessment of contamination, it may obscure localised variations, especially in vertically differentiated soil systems. Similar limitations of complex indices based on aggregated values have been noted in previous studies, which emphasise that such indices can mask element-specific or horizon-specific anomalies. Therefore, although the PLI is effective for the general classification of soil quality, it should be interpreted with caution when assessing the spatial or vertical variability of contamination, and preferably used in combination with more sensitive indices [41,63].

On the other hand, it should be noted that some soils located in embankments may also show enrichment with heavy metals, as reported by Gmitrowicz-Iwan et al. [78], who found that, during floods, sediment containing high levels of heavy metals can be carried away by flowing water, leading to river pollution. Conversely, during droughts, these sediments can transform into soils, potentially increasing heavy metal availability within the embankment area. This scenario could be reflected in the pollution classes obtained for the studied fluvisols from Group 2.

The RI values, however, showed that, regardless of location (inter-embankment vs. out of embankment), the surface horizons were the most polluted (Figure 6). Similar results in the case of potential ecological risk have been noted by Kobierski [45], who connected these findings with the higher content of TOC in the surface layer. On the other hand, surface layers are susceptible to the continuous influx of new pollutants, which are often rich in heavy metals. Meanwhile, in lower soil layers, pollutants can migrate deeper into the soil profile or be eroded [86].

The study results indicate that standard soil monitoring in river valleys should move away from simplified aggregate indices and toward indices that take into account the specificity of the soil profile (e.g., PIN or RI). This avoids errors in soil classification, which, although appearing similar in terms of the PLI, exhibit significantly different toxicity in the subsurface layers. The precise identification of the degree of contamination using the RI index allows for the differentiation of management strategies. In the inter-embankment zone, the results suggest the need to restrict agricultural use (animal grazing) at points with the highest RI to prevent the transfer of metals into the food chain during floods. In the embankment zone, the results can serve as a basis for designating safe cultivation zones with low metal accumulation.

5. Conclusions

- Comparative soil analyses found higher heavy metal contents in the inter-embankment zone, which likely resulted from the continuous supply of mineral material. The elevated heavy metal contents therefore represent a genetic characteristic of fluvisols.
- The vertical distribution of heavy metals in the analysed fluvisols is primarily influenced by the gradual deposition of alluvial material, often enriched with industrial and municipal pollutants, as well as by the inherent chemical and physical properties of the soils. This leads to irregular vertical patterns, with no consistent decreasing trend towards the bottom of the soil profiles, particularly in layers of silty-loam and loam deposited by the river in the middle profile sections.
- The vertical distribution of pollutants is closely related to the dynamics of alluvial material deposition and the physicochemical properties of soils. The clay fraction, organic matter content and redox conditions play a key role here.

https://doi.org/10.3390/su18125996

- Regardless of the depth of the profile, accumulation processes occur most intensively in fine-grained layers. The presence of silty and loamly layers deposited by the river in the central parts of the profile means that there is no clear downward trend in metal concentrations with depth.
- The silty loam and loam, higher organic matter content, and redox conditions contributed to elevated concentrations of the examined heavy metals in the surface horizons, which was confirmed by the values of the PI, PIN and RI pollution indices.
- The PLI pollution index indicated a deterioration in soil quality in both the inter-embankment zone and out of the embankment, with relatively similar contamination classes. This result reflects the characteristics of the applied pollution indices. Owing to their stratified nature, fluvisols may exhibit substantial variability in contamination classes within a single soil profile, which may not be fully captured by indices such as the PLI because of their broad classification scale.
- The results demonstrate that the selection of an appropriate pollution index is crucial for assessing heavy metal contamination in fluvisols. Among the indices applied, the PI, PIN and RI most accurately reflected the actual degree of contamination of fluvisols in the Middle Odra Valley.

Supplementary Materials: The following supporting information can be downloaded at: https://www.mdpi.com/article/10.3390/su18125996/s1, Table S1: Pollution indices; Table S2: Total concentrations of potentially toxic elements in the studied soils.

Author Contributions: Conceptualization, D.K. and J.B.K.; methodology, D.K., J.K. and J.B.K.; software, J.K. and J.B.K.; validation, J.B.K., J.K. and D.K.; formal analysis, D.K., J.B.K. and M.K.; investigation, D.K., P.J. and D.S.; resources, D.K.; data curation, D.K.; writing—original draft preparation, D.K. and J.B.K.; writing—review and editing, D.K., J.B.K., J.K., P.J., D.S., M.K. and J.G.-I.; visualisation, D.K., J.B.K. and P.J.; supervision, D.K. and J.B.K.; supervision, D.K.; funding acquisition, D.K. All authors have read and agreed to the published version of the manuscript.

Funding: This research was financed by Wroclaw University of Environmental and Life Sciences from the statutory funds for research.

Institutional Review Board Statement: Not applicable.

Informed Consent Statement: Not applicable.

Data Availability Statement: Data from this study is available upon request.

Conflicts of Interest: The authors declare no conflicts of interest.

Appendix A

Table A1. Pollution indices.

Index	Description	Formula	Explanation	Limitation	Pollution Class
Single Pollution Index (*PI*)	*PI* helps to determine the presence of heavy metal contamination [41,60]	$PI = \frac{C}{B}$	C_i—determined heavy metal content in soil horizon; *B*—local and reference geochemical background used in this study.	PI is simple to calculate and widely used for evaluating individual element contamination relative to the geochemical background (GB). However, it does not account for the natural variability of heavy metal concentrations, and its accuracy strongly depends on the correct selection of GB values [41]. Misestimation of local background can lead to over- or underestimation of contamination.	Class / Range / Interpretation 1 / <1 / absent 2 / $<1 < PI < 2$ / low 3 / $<2 < PI < 3$ / moderate 4 / $<3 < PI < 5$ / strong 5 / $PI > 5$ / very strong
Background Enrichment Factor (*PIN*)	*PIN* allows for overall assessment of heavy metal content in studied soils [40,61]	$PIN = \sum_{i=1}^{n} \frac{PIClass^2 \times Cn}{GB}$	*PIClass*—class of *PI*; *Cn*—contamination by heavy metal; GB—geochemical background.	PIN integrates multiple PI values into a single index, reflecting overall contamination. Its main strength is the integration of all analysed elements into a single metric with a precise scale. Nevertheless, it does not consider natural geochemical processes and requires prior classification of PI values, which may introduce some subjectivity in interpretation.	0–7—clean 7–95.1—trace contamination 95.1–518.1—lightly contaminated 518.1–2548.5—contaminated ≥2548.8—highly contaminated

Table A1. *Cont.*

Index	Description	Formula	Explanation	Limitation	Pollution Class
Potential Ecological Risk (*RI*)	*RI* is used for potential ecological and environmental risk as well as contamination assessment caused by a concentration of heavy metals both in water and air, as well as in soil according to Håkanson [62].	$RI = \sum_{i=1}^{m} Er^i$ $E_r^i = T_r^i x PI$	E_r—single index of ecological risk factor; m—number of studied heavy metals; $T_r{}^i$—the toxicity response coefficient of heavy metals; PI—single pollution index of heavy metal using reference geochemical background. The $T_r{}^i$ values applied in this study are presented in Table A4: Hg—40; Cd—30; As—10; Cu—5; Pb—5; Cr—2; Zn—2; Ni—5.	RI evaluates potential ecological risk by incorporating toxicity and ecological sensitivity of individual metals. Its advantage is the comprehensive assessment of ecological implications rather than only concentration levels. However, RI requires toxic-response factors, which are only available for certain elements, and it does not use LGB values. The ranking system of individual element risks can also introduce uncertainty in interpretation.	Classes of *RI* according to Håkanson [62]: ≤90: low 90–180: moderate 180–360: strong 360–720: very strong ≥720: highly strong
Pollution Load Index (*PLI*)	This indicator provides an easy way to show the deterioration in the soil as a result of the accumulation of heavy metals [41,63].	$PLI = \sqrt[n]{PI_1 \times PI_2 \times PI_3 \times \ldots PI_n}$	n—number of analysed heavy metals; PI—calculated values of Single Pollution Index.	PLI provides an overall assessment of site contamination, allowing easy comparison between different locations. Similar to PI and PIN, it does not account for natural geochemical variability, and the accuracy of PLI depends on the choice of geochemical background. Additionally, PLI may mask the contribution of highly enriched individual elements, which could be important in ecological or health risk evaluations.	<1 denotes perfection 1 denotes only baseline levels of pollution >1 denotes deterioration of soil quality

Appendix B

Table A2. Total concentrations of potentially toxic elements in the studied soils.

Profile Number	Horizon	Depth (cm)	Cd $mg \cdot kg^{-1}$	Cu	Zn	Pb
P1 In-E	Ad	0–10	2.36	22.1	101.0	35.48
	ABwg	10–20	1.52	18.1	75.5	22.58
	Bwg	20–45	0.62	20.4	54.0	13.95
	BCg	45–55	0.58	18.9	43.9	13.04
	IIG	55–58	0.79	7.38	13.9	4.74
	IIIG1	58–75	0.68	17.9	45.9	13.75
	IIIG2	75–85	0.57	16.9	43.4	13.69
	IVG1	85–100	0.43	2.38	5.38	2.27
	IVG2	100–130	0.40	1.38	3.88	1.92
P2 In-E	Ad	0–18	2.25	36.4	263	50.27
	ABw	18–30	1.45	21.9	173	44.06
	Bwg1	30–52	0.69	12.4	45.35	13.14
	Bwg2	52–80	0.70	10.9	55.35	14.28
	BCg	80–100	0.63	9.35	43.85	11.72
	IICg1	100–113	0.59	7.35	33.85	7.86
	IICg2	113–122	0.86	11.9	53.35	11.78
	IICgg	122–135	0.44	5.35	23.85	6.61
	IIICgg	135–160	0.40	3.35	12.35	3.86
P3 In-E	Ad	0–18	2.30	41.4	256	51.02
	ABw	18–28	1.51	23.4	178	39.23
	Bwg1	28–40	0.73	12.4	53.35	16.39
	Bwg2	40–70	0.65	10.9	35.35	11.77
	Bwg3	70–86	0.68	9.85	40.35	12.16
	Cg	86–103	0.65	8.35	34.85	11.67
	IICg	103–150	0.40	2.35	15.35	4.81

Table A2. *Cont.*

Profile Number	Horizon	Depth (cm)	Cd mg·kg^{-1}	Cu	Zn	Pb
P3 In-E	IIIG	150–175	0.40	1.35	13.85	3.15
	IVCgg	175–190	0.40	<LoD	3.35	1.41
P4 Out E	Ap	0–30	0.78	9.38	39.9	15.68
	IIBvg	30–45	0.65	0.88	8.88	2.77
	IIBvCg	45–60	0.67	<LoD	6.88	2.18
	IICg1	60–72	0.59	<LoD	2.38	1.21
	IICg2	72–78	0.45	0.38	11.4	3.47
	IICg3	78–110	0.47	<LoD	2.88	1.24
	IICgg	110–130	0.40	<LoD	4.88	1.31
P5 Out E	Ap	0–24	0.55	6.63	15.5	17.56
	ABv	24–40	0.46	3.63	10.5	10.01
	IICrg1	40–60	0.40	1.13	20.0	4.26
	IICrg2	60–90	0.49	0.63	5.00	3.64
	IICrg3	90–115	0.42	0.63	3.50	1.99
	IIG	115–150	0.40	0.63	7.00	2.35
	IIIG	150–180	0.40	4.13	14.5	4.83
P6 Out E	Ap	0–33	0.86	7.38	32.9	12.97
	IIBv	33–55	0.83	1.88	12.9	4.74
	IICg1	55–70	0.75	4.35	6.35	19.57
	IIC2	70–90	0.95	1.85	2.35	1.39
	IIC3	90–110	0.43	1.35	3.85	1.73
	IIC4	110–130	0.40	<LoD	2.85	1.45

Explanation: In-E—inter-embankment; Out E—out of embankment; <LoD—below the limit of detection.

Appendix C

Table A3. Comparison of average metal and TOC contents in IN-E and OUT-E soil profiles at corresponding depths.

Compared Average Depth [cm] IN-E/OUT-E	Cd [mg·kg^{-1}]		Cu [mg·kg^{-1}]		Zn [mg·kg^{-1}]		Pb [mg·kg^{-1}]		TOC [g·kg^{-1}]	
11.0/14.5	2.02 *	0.73 *	31.97	7.79	198.17	29.42	41.29	15.40	42.12	10.60
	0.021 *		0.030		0.052		0.044		0.062	
30.2/37.8	0.93	0.65	18.23	2.13	93.45	10.75	24.80	5.84	16.16	3.1
	0.793		0.017		0.020		0.003		0.025	
48.7/55.0	0.64	0.61	14.07	1.89	41.53	11.08	12.65	8.67	8.02	1.51
	0.374		0.065		0.023		0.180		0.017	
70.2/73.7	0.69	0.68	12.88	0.89	47.20	3.24	13.39	2.08	7.45	0.89
	0.268		0.033		0.002		0.012		0.002	
104.3/92.5	0.52	0.43	8.87	0.78	30.87	6.24	8.78	2.39	5.03	1.08
	0.154		0.069		0.016		0.004		0.064	
129.2/128.3	0.41	0.41	2.76	1.07	11.86	6.42	3.56	2.23	1.80	0.73
	0.484		0.013		0.084		0.037		0.026	

* average content IN-E.

Table A4. Correlation coefficients for the IN-E area.

	In-E (n = 27)					
	Depth	Cd	Cu	Zn	Pb	TOC
Cd	−0.735	x				
Cu	−0.812	0.850	x			
Zn	−0.678	0.880	0.912	x		
Pb	−0.764	0.924	0.919	**0.973**	x	
TOC	−0.674	0.926	0.906	**0.980**	0.958	x
clay	−0.355	0.273	0.366	0.156	0.220	0.151

Explanation: Statistically significant correlations (at the p = 0.05 level) are marked in red.

Table A5. Correlation coefficients for the OUT-E area.

	Out E (n = 20)					
	Depth	Cd	Cu	Zn	Pb	TOC
Cd	−0.577	x				
Cu	−0.525	0.456	x			
Zn	−0.545	0.354	0.826	x		
Pb	−0.588	0.382	0.861	0.603	x	
TOC	−0.696	0.477	0.879	0.878	0.697	x
clay	−0.268	0.320	0.766	0.873	0.448	0.789

Explanation: Statistically significant correlations (at the p = 0.05 level) are marked in red.

Table A6. Correlation coefficients for the IN-E area and OUT-E area.

	In-E and Out E (n = 47)					
	Depth	Cd	Cu	Zn	Pb	TOC
Cd	−0.620	x				
Cu	−0.574	0.825	x			
Zn	−0.515	0.868	0.919	x		
Pb	−0.629	0.888	0.915	0.947	x	
TOC	−0.563	0.912	0.904	0.977	0.943	x
clay	−0.245	0.346	0.610	0.407	0.435	0.383

Explanation: Statistically significant correlations (at the p = 0.05 level) are marked in red.

Appendix D

Table A7. Total stock of metals and TOC in the described soil layers in the IN-E and OUT-E soil profiles.

Soil Layer	IN-E	OUT-E	p (T $\leq$ t) One-Tailed p-Value
	Total Cd Stocks in Soil Layer (mg)		
0–50	**866**	**439**	**0.023**
50–100	478	442	0.332
100–150	317	286	0.224
	Total Cu stocks in soil layer (mg)		
0–50	**14,839**	**3272**	**0.002**
50–100	**8176**	**862**	**0.010**
100–150	2635	314	0.079
	Total Zn stocks in soil layer (mg)		
0–50	**79,120**	**14,133**	**0.037**
50–100	**27,600**	**4008**	**0.010**
100–150	11,366	3144	0.110

https://doi.org/10.3390/su18125996

Table A7. *Cont.*

Soil Layer	IN-E	OUT-E	p (T ≤ t) One-Tailed p-Value
Total Pb stocks in soil layer (mg)			
0–50	**18,689**	**6845**	**0.021**
50–100	**8108**	**2884**	**0.019**
100–150	3308	1176	0.068
Total TOC stocks in soil layer (g)			
0–50	**15,812**	**4546**	**0.044**
50–100	**4445**	**763**	**0.019**
100–150	1934	421	0.139

References

1. Nilsson, C.; Berggren, K. Alterations of riparian ecosystems caused by river regulation. *BioScience* **2000**, *50*, 783–792. [CrossRef]
2. Halarewicz, A.; Pruchniewicz, D.; Kawałko, D. Using Direct and Indirect Methods to Assess Changes in Riparian Habitats. *Forests* **2021**, *12*, 504. [CrossRef]
3. Kabała, C. Origin, transformation and classification of alluvial soils (mady) in Poland—Soils of the year 2022. *Soil Sci. Annu.* **2022**, *73*, 156043. [CrossRef]
4. Dezső, J.; Czigány, S.; Nagy, G.; Pirkhoffer, E.; Słowik, M.; Lóczy, D. Monitoring soil moisture dynamics in multilayered Fluvisols. *Bull. Geogr. Phys. Geogr. Ser.* **2019**, *16*, 131–146. [CrossRef]
5. Kercheva, M.; Sokołowska, Z.; Hajnos, M.; Skic, K.; Shishkov, T. Physical parameters of Fluvisols on flooded and non-flooded terraces. *Int. Agrophys.* **2017**, *31*, 73–82. [CrossRef]
6. Gajić, B.; Kresović, B.; Pejić, B.; Tapanarova, A.; Dugalić, G.; Životić, L.; Sredojević, Z.; Tolimir, M. Some physical properties of long-term irrigated fluvisols of valley the river Beli Drim in Klina (Serbia). *Zemljište I Biljka* **2020**, *69*, 21–35. [CrossRef]
7. Andrés-Doménech, I.; García-Bartual, R.; Montanari, A.; Marco, J.B. Climate and hydrological variability: The catchment filtering role. *Hydrol. Earth Syst. Sci.* **2015**, *19*, 379–387. [CrossRef]
8. Bawden, A.J.; Burn, D.H.; Prowse, T.D. Recent changes in patterns of western Canadian river flow and association with climatic drivers. *Hydrol. Res.* **2015**, *46*, 551–565. [CrossRef]
9. Ligęza, S. Variability of the Contemporary Fluvisols of the Vistula River near Puławy. *Sci. Diss. Lub. Univ. Life Sci.* **2016**, *385*, 1–131.
10. Hulisz, P.; Michalski, A.; Dąbrowski, M.; Kusza, G.; Łęczyński, L. Human-induced changes in the soil cover at the mouth of the Vistula River Cross-Cut (northern Poland). *Soil Sci. Annu.* **2015**, *66*, 67–74. [CrossRef]
11. Pływaczyk, L. *The Impact of River Damming on Valley on the Example of Brzeg Dolny. Monograph No. 11*; Wrocław Agricultural University: Wrocław, Poland, 1997.
12. Głuchowska, B.; Pływaczyk, L. Groundwater Level in the Odra River Valley Downstream the Brzeg Dolny. *Contemp. Probl. Environ. Eng.* **2008**, *5*, 1–109.
13. Kawałko, D.; Kaszubkiewicz, J.; Jezierski, P. Morphology and selected properties of alluvial soils in the Odra River valley, SW Poland. *Soil Sci. Annu.* **2022**, *73*, 156062. [CrossRef]
14. Laskowski, S. Origin, evolution and the properties of alluvial soils from the middle Odra River-valley. *Sci. Pap. Wrocław. Agric. Univ.* **1986**, *56*, 1–68.
15. Frohne, T.; Rinklebe, J.; Diaz-Bone, R.A. Contamination of Floodplain Soils along the Wupper River, Germany, with As, Co, Cu, Ni, Sb, and Zn and the Impact of Pre-definite Redox Variations on the Mobility of These Elements. *Soil Sediment Contam. Int. J.* **2014**, *23*, 779–799. [CrossRef]
16. Marrugo-Negrete, J.; Pinedo-Hernández, J.; Díez, S. Assessment of heavy metal pollution, spatial distribution and origin in agricultural soils along the Sinú River Basin, Colombia. *Environ. Res.* **2017**, *154*, 380–388. [CrossRef] [PubMed]
17. Pan, L.; Fang, G.; Wang, Y.; Wang, L.; Su, B.; Li, D.; Xiang, B. Potentially Toxic Element Pollution Levels and Risk Assessment of Soils and Sediments in the Upstream River, Miyun Reservoir, China. *Int. J. Environ. Res. Public Health* **2018**, *15*, 2364. [CrossRef] [PubMed]
18. Wang, J.; Lautz, L.S.; Nolte, T.M.; Posthuma, L.; Koopman, K.R.; Leuven, R.S.; Hendriks, A.J. Towards a systematic method for assessing the impact of chemical pollution on ecosystem services of water systems. *J. Environ. Manag.* **2021**, *281*, 111873. [CrossRef]

19. Kanianska, R.; Varga, J.; Benková, N.; Kizeková, M.; Jančová, L'. Floodplain soils contamination assessment using the sequential extraction method of heavy metals from past mining activities. *Sci. Rep.* **2022**, *12*, 2927. [CrossRef]
20. Ciszewski, D.; Grygar, M. A Review of Flood-Related Storage and Remobilization of Heavy Metal Pollutants in River Systems. *Water Air Soil Pollut.* **2016**, *227*, 239. [CrossRef] [PubMed]
21. Heritage, G.; Entwistle, N. Impacts of River Engineering on River Channel Behaviour: Implications for Managing Downstream Flood Risk. *Water* **2020**, *12*, 1355. [CrossRef]
22. Rinklebe, J.; Shaheen, S.M. Assessing the mobilization of cadmium, lead, and nickel using a seven-step sequential extraction technique in contaminated floodplain soil profiles along the Central Elbe River, Germany. *Water Air Soil Pollut.* **2014**, *225*, 2039. [CrossRef]
23. Shaheen, S.M.; Antoniadis, V.; Kwon, E.; Song, H.; Wang, S.-L.; Hseu, Z.-Y.; Rinklebe, J. Soil contamination by potentially toxic elements and the associated human health risk in geo- and anthropogenic contaminated soils: A case study from the temperate region (Germany) and the arid region (Egypt). *Environ. Pollut.* **2020**, *262*, 114312. [CrossRef]
24. Kotková, K.; Nováková, T.; Tůmová, Š.; Kiss, T.; Popelka, J.; Faměra, M. Migration of risk elements within the floodplain of the Litavka River, the Czech Republic. *Geomorphology* **2019**, *329*, 46–57. [CrossRef]
25. Shaheen, S.M.; Rinklebe, J.; Selim, M.H. Impact of various amendments on immobilization and phytoavailability of nickel and zinc in a contaminated floodplain soil. *Int. J. Environ. Sci. Technol.* **2015**, *12*, 2765–2776. [CrossRef]
26. Absalon, D.; Matysik, M. Changes in water quality and runoff in the Upper Oder River Basin. *Geomorphology* **2007**, *92*, 106–118. [CrossRef]
27. Aleksander-Kwaterczak, U.; Helios-Rybicka, E. Contaminated sediments as a potential source of Zn, Pb, and Cd for a river system in the historical metalliferous ore mining and smelting industry area of South Poland. *J. Soils Sediments* **2009**, *9*, 13–22. [CrossRef]
28. Ciszewski, D.; Turner, J. Storage of sediment-associated heavy metals along the channelized Odra River, Poland. *Earth Surf. Process. Landf.* **2009**, *34*, 558–572. [CrossRef]
29. Strzebońska, M.; Jarosz-Krzemińska, E.; Adamiec, E. Assessing Historical Mining and Smelting Effects on Heavy Metal Pollution of River Systems over Span of Two Decades. *Water Air Soil Pollut.* **2017**, *228*, 141. [CrossRef]
30. Faměra, M.; Matys Grygar, T.; Ciszewski, D.; Czajka, A.; Álvarez-Vázquez, M.Á.; Hron, K.; Fačevicová, K.; Hýlová, V.; Tůmová, Š.; Světlík, I.; et al. Anthropogenic records in a fluvial depositional system: The Odra River along The Czech-Polish border. *Anthropocene* **2021**, *34*, 100286. [CrossRef]
31. Czaja, S. Changes in river discharge structure and regime in mining-industrial-urban areas. *Reg. Environ. Change* **2005**, *5*, 18–26. [CrossRef]
32. Ciszewski, D.; Czajka, A. Human-induced sedimentation patterns of a channelized lowland river. *Earth Surf. Process. Landf.* **2015**, *40*, 783–795. [CrossRef]
33. Lis, J.; Pasieczna, A. *Geochemical Atlas of Poland. 1:2 500 000*; National Geological Institute: Daejeon, Republic of Korea, 1995.
34. Bojakowska, I.; Sokołowska, G. Influence of ore mining and metallurgy for pollution of the Odra River alluvial deposits with trace elements. *Przegl. Geol.* **1998**, *46*, 603–608.
35. Gielar, A.; Helios-Rybicka, E.; Möller, S.; Einax, J.W. Multivariate analysis of sediment data from the upper and middle Odra River (Poland). *Appl. Geochem.* **2012**, *27*, 1540–1545. [CrossRef]
36. Ciszewski, D. Heavy metals in vertical profiles of the middle Odra River overbank sediments: Evidence for pollution changes. *Water Air Soil Pollut.* **2003**, *143*, 81–98. [CrossRef]
37. Karczewska, A.; Kaszubkiewicz, J.; Kabała, C.; Jezierski, P.; Spiak, Z.; Szopka, K. Chapter 6-Tailings Impoundments of Polish Copper Mining Industry—Environmental Effects, Risk Assessment and Reclamation. *Assess. Restor. Reclam. Min. Influ. Soils* **2017**, 149–202. [CrossRef]
38. Kawałko, D.; Karczewska, A.; Lewińska, K. Environmental risk associated with accumulation of toxic metalloids in soils of the Odra River floodplain-case study of the assessment based on total concentrations, fractionation and geochemical indices. *Environ. Geochem. Health* **2023**, *45*, 4461–4476. [CrossRef]
39. Kawałko, D.; Karczewska, A. Profile Distributions of Potentially Toxic Metal(loid)s in Soils of the Middle Odra Floodplain (SW Poland). *Int. J. Environ. Res. Public Health* **2023**, *20*, 4196. [CrossRef] [PubMed]
40. Gong, Q.; Deng, J.; Xiang, Y.; Wang, Q.; Yang, L. Calculating Pollution Indices by Heavy Metals in Ecological Geochemistry Assessment and a Case Study in Parks of Beijing. *J. China Univ. Geosci.* **2008**, *19*, 230–241. [CrossRef]
41. Kowalska, J.B.; Mazurek, R.; Gąsiorek, M.; Zaleski, T. Pollution indices as useful tools for the comprehensive evaluation of the degree of soil contamination–A review. *Environ. Geochem. Health* **2018**, *40*, 2395–2420. [CrossRef] [PubMed]
42. Swain, C.K. Environmental pollution indices: A review on concentration of heavy metals in air, water, and soil near industrialization and urbanisation. *Discov. Environ.* **2024**, *2*, 5. [CrossRef]
43. Wieczorek, K.; Turek, A.; Szczesio, M.; Wolf, W.M. Comprehensive Evaluation of Metal Pollution in Urban Soils of a Post-Industrial City—A Case of Łódź, Poland. *Molecules* **2020**, *25*, 4350. [CrossRef] [PubMed]

44. Adewumi, A.J.; Ogundele, O.D. Hidden hazards in urban soils: A meta-analysis review of global heavy metal contamination (2010–2022), sources and its Ecological and health consequences. *Sustain. Environ.* **2023**, *10*, 2293239. [CrossRef]
45. Kobierski, M. Evaluation of the Content of Heavy Metals in Fluvisols of Floodplain Area Depending on the Type of Land Use. *J. Ecol. Eng.* **2015**, *16*, 23–31. [CrossRef]
46. Glina, B.; Kowalska, J.B.; Łuczak, K.; Mazurek, R.; Spychalski, W.; Mendyk, Ł. Potentially toxic elements in fen peatland soils located near lignite-fired power plants in Central Poland. *Geoderma Reg.* **2021**, *25*, e00370. [CrossRef]
47. Smirnova, T.S.; Mazlova, E.A.; Kulikova, O.A.; Ostrovkin, I.M.; Gonopolsky, A.M.; Cheloznova, K.V. Chemical and biological indicators for evaluation of Arctic soil degradation and its potential to remediation. *J. Environ. Eng. Landsc. Manag.* **2021**, *29*, 33–39. [CrossRef]
48. Gąsiorek, M.; Kowalska, J.; Mazurek, R.; Pająk, M. Comprehensive assessment of heavy metal pollution in topsoil of historical urban park on an example of the Planty Park in Krakow (Poland). *Chemosphere* **2017**, *179*, 148–158. [CrossRef]
49. Marks, L. Quaternary Glaciations in Poland. *Dev. Quat. Sci.* **2011**, *15*, 299–303. [CrossRef]
50. Kabała, C. (Ed.) *Soils of Lower Silesia. Origins, Diversity and Protection*; Polish Society of Soil Science: Warsaw, Poland, 2015.
51. IUSS Working Group WRB. World Reference Base for Soil Resources. In *International Soil Classification System for Naming Soils and Creating Legends for Soil Maps*, 4th ed.; International Union of Soil Sciences: Rome, Italy, 2022.
52. Papuga, K.; Kaszubkiewicz, J.; Wilczewski, W.; Staś, M.; Belowski, J.; Kawałko, D. Soil grain size analysis by the dynamometer method—A comparison to the pipette and hydrometer method. *Soil Sci. Annu.* **2018**, *69*, 17–27. [CrossRef]
53. Tan, K. *Soil Sampling, Preparation, and Analysis*, 2nd ed.; CRC Press: Boca Raton, FL, USA, 2005.
54. *ISO 11466*; Soil Quality. Extraction of Trace Elements Soluble in Aqua Regia. International Organization for Standardization: Geneva, Switzerland, 1995.
55. Gao, X.; Chen, C.T.A. Heavy metal pollution status in surface sediments of the coastal Bohai Bay. *Water Res.* **2012**, *46*, 1901–1911. [CrossRef] [PubMed]
56. Kowalska, J.B.; Gąsiorek, M.; Zadrożny, P.; Nicia, P.; Waroszewski, J. Deep Subsoil Storage of Trace Elements and Pollution Assessment in Mountain Podzols (Tatra Mts., Poland). *Forests* **2021**, *12*, 291. [CrossRef]
57. Askari, M.S.; Alamdari, P.; Chahardoli, S.; Afshari, A. Quantification of heavy metal pollution for environmental assessment of soil condition. *Environ. Monit. Assess.* **2020**, *192*, 162. [CrossRef]
58. Hołtra, A.; Zamorska-Wojdyła, D. The pollution indices of trace elements in soils and plants close to the copper and zinc smelting works in Poland's Lower Silesia. *Environ. Sci. Pollut. Res.* **2020**, *27*, 16086–16099. [CrossRef]
59. Li, Y.; Abuduwaili, J.; Ma, L.; Liu, W.; Zeng, T. Source apportionment and source-specific risk evaluation of potential toxic elements in oasis agricultural soils of Tarim River Basin. *Sci. Rep.* **2023**, *13*, 2980. [CrossRef]
60. Guan, Y.; Shao, C.; Ju, M. Heavy Metal Contamination Assessment and Partition for Industrial and Mining Gathering Areas. *Int. J. Environ. Res. Public Health* **2014**, *11*, 7286–7303. [CrossRef] [PubMed]
61. Caeiro, S.; Costa, M.H.; Ramos, T.B.; Fernandes, F.; Silveira, N.; Coimbra, A.; Medeiros, G.; Painho, M. Assessing heavy metal contamination in Sado Estuary sediment: An index analysis approach. *Ecol. Indic.* **2005**, *5*, 151–169. [CrossRef]
62. Hakanson, L. An ecological risk index for aquatic pollution control.a sedimentological approach. *Water Res.* **1980**, *14*, 975–1001. [CrossRef]
63. Varol, M. Assessment of heavy metal contamination in sediments of the Tigris River (Turkey) using pollution indices and multivariate statistical techniques. *J. Hazard. Mater.* **2011**, *195*, 355–364. [CrossRef]
64. Reimann, C.; Garrett, R.G. Geochemical background—Concept and reality. *Sci. Total Environ.* **2005**, *350*, 12–27. [CrossRef]
65. Kobierski, M.; Dabkowska-Naskret, H. Local background concentration of heavy metals in various soil types formed from glacial till of the Inowrocławska plain. *J. Elem.* **2012**, *17*, 559–585. [CrossRef]
66. Macklin, M.G.; Benito, G.; Gregory, K.J.; Johnstone, E.; Lewin, J.; Michczyńska, D.; Soja, R.; Starkel, L.; Thorndycraft, V. Past hydrological events reflected in the Holocene fluvial record of Europe. *Catena* **2006**, *66*, 145–154. [CrossRef]
67. Du Laing, G.; Rinklebe, J.; Vandecasteele, B.; Meers, E.; Tack, F.M.G. Trace metal behaviour in estuarine and riverine floodplain soils and sediments: A review. *Sci. Total Environ.* **2009**, *407*, 3972–3985. [CrossRef]
68. Łabaz, B.; Bogacz, A.; Kabała, C. Anthropogenic transformation of soils in the Barycz valley—Conclusions for soil classification / Antropogeniczne przekształcenia gleb w Dolinie Baryczy-wnioski dotyczące klasyfikacji gleb. *Soil Sci. Annu.* **2014**, *65*, 103–110. [CrossRef]
69. Regulation of the Minister for the Environment of 1 September 2016 on the Method How to Carry out the Assessment of Soil Contamination. Polish Journal of Laws Item 1395, 2016. (In Polish)
70. Karczewska, A.; Kabała, C. Environmental risk assessment as a new basis for evaluation of soil contamination in Polish law. *Soil Sci. Annu.* **2017**, *68*, 67–80. [CrossRef]
71. Li, Y.; Wang, K.; Dötterl, S.; Xu, J.; Garland, G.; Liu, X. The critical role of organic matter for cadmium-lead interactions in soil: Mechanisms and risks. *J. Hazard. Mater.* **2024**, *476*, 135123. [CrossRef]

72. Harmsen, J. Measuring Bioavailability: From a Scientific Approach to Standard Methods. *J. Environ. Qual.* **2007**, *36*, 1420–1428. [CrossRef]
73. Saint-Laurent, D.; Lavoie, L.; Drouin, A.; St-Laurent, J.; Ghaleb, B. Floodplain sedimentation rates, soil properties and recent flood history in southern Québec. *Glob. Planet. Change* **2010**, *70*, 76–91. [CrossRef]
74. Ciszewski, D.; Czajka, A.; Błażej, S. Rapid migration of heavy metals and 137 Cs in alluvial sediments, Upper Odra River valley, Poland. *Environ. Geol.* **2008**, *55*, 1577–1586. [CrossRef]
75. van Gestel, C.A.M. Physico-chemical and biological parameters determine metal bioavailability in soils. *Sci. Total Environ.* **2008**, *406*, 385–395. [CrossRef]
76. Mao, L.; Kong, H.; Li, F.; Chen, Z.; Wang, L.; Lin, T.; Lu, Z. Improved geochemical baseline establishment based on diffuse sources contribution of potential toxic elements in agricultural alluvial soils. *Geoderma* **2022**, *410*, 115669. [CrossRef]
77. Matschullat, J.; Ellminger, F.; Agdemir, N.; Cramer, S.; Ließmann, W.; Niehoff, N. Overbank sediment profiles—Evidence of early mining and smelting activities in the Harz mountains, Germany. *Appl. Geochem.* **1997**, *12*, 105–114. [CrossRef]
78. Gmitrowicz-Iwan, J.; Ligęza, S.; Pranagal, J.; Kołodziej, B.; Smal, H. Can climate change transform non-toxic sediments into toxic soils? *Sci. Total Environ.* **2020**, *747*, 141201. [CrossRef]
79. Dennis, I.A.; Coulthard, T.J.; Brewer, P.; Macklin, M.G. The role of floodplains in attenuating contaminated sediment fluxes in formerly mined drainage basins. *Earth Surf. Process. Landf.* **2009**, *34*, 453–466. [CrossRef]
80. Foulds, S.A.; Brewer, P.A.; Macklin, M.G.; Haresign, W.; Betson, R.E.; Rassner, S.M.E. Flood-related contamination in catchments affected by historical metal mining: An unexpected and emerging hazard of climate change. *Sci. Total Environ.* **2014**, *476–477*, 165–180. [CrossRef] [PubMed]
81. Suresh, G.; Sutharsan, P.; Ramasamy, V.; Venkatachalapathy, R. Assessment of spatial distribution and potential ecological risk of the heavy metals in relation to granulometric contents of Veeranam lake sediments, India. *Ecotoxicol. Environ. Saf.* **2012**, *84*, 117–124. [CrossRef] [PubMed]
82. Çevik, F.; Göksu, M.Z.L.; Derici, O.B.; Fındık, Ö. An assessment of metal pollution in surface sediments of Seyhan dam by using enrichment factor, geoaccumulation index and statistical analyses. *Environ. Monit. Assess.* **2009**, *152*, 309–317. [CrossRef]
83. Alloway, B.J. *Heavy Metals in Soils. Trace Metals and Metalloids in Soils and Their Bioavailability*, 3rd ed.; Alloway, B.J., Ed.; Springer: Dordrecht, The Netherlands, 2013; Volume 22. [CrossRef]
84. Kabata-Pendias, A.; Szteke, B. *Trace Elements in Abiotic and Biotic Environments*; Taylor & Francis: Abingdon, UK, 2015.
85. Caporale, A.G.; Violante, A. Chemical Processes Affecting the Mobility of Heavy Metals and Metalloids in Soil Environments. *Curr. Pollut. Rep.* **2016**, *2*, 15–27. [CrossRef]
86. Kumar, V.; Sharma, A.; Kaur, P.; Sidhu, G.P.S.; Bali, A.S.; Bhardwaj, R.; Thukral, A.K.; Cerda, A. Pollution assessment of heavy metals in soils of India and ecological risk assessment: A state-of-the-art. *Chemosphere* **2019**, *216*, 449–462. [CrossRef]